Contact of screw machine rotors under operate loading

Ass. Prof. J. Švígler, University of West Bohemia, Pilsen;

Ing. V. Machulda, University of West Bohemia, Pilsen;

Abstract

Rotors of a liquid injected screw machines create a pair of conjugate screw surfaces that touch mutually. Force and temperature loading of the screw machine housing causes a change in an arrangement of the rotor axes. An originally parallel ordering changes into a space arrangement with the skew axes. This change causes a variation of the character contact of tooth surfaces. The curve contact degenerates into the point contact. The change of the surface contact produces another phenomenon such as arise of undesirable gaps between tooth surfaces, change of the gear ratio and static and dynamic stress of surfaces. Presented contribution analyses the incorrect contact of screw surfaces of the rotors in detail. Problem is solved as a three-dimensional case.

1. Introduction

Screw machines with liquid injection into the compressed gas, which operate with high pressure differences, are heavily loaded by axial and radial forces [2], [3], which are transferred to the housing by the bearings. The contact force between the rotors Fig. 1, play an important role in screw machines with direct rotor contact. The contact force is relatively smaller in the case of a main rotor driven compressor. In the case of a gate rotor drive the contact force is substantially larger and this case, which comes into account by screw expanders, is excluded from our consideration. This statement is valid for a curve contact of rotor tooth surfaces which are located in a theoretical, unloaded, position. In the case of a point contact the contact force is substantially larger. The curve contact changes in the contact at the point in a housing distortion when an originally parallel position of rotor axes changes in a space arrangement with skew axes. The distortion is caused by the force and temperature fields and by an

Fig. 1 Screw machine rotors

operational vibration. Decesive influence on the housing distortion has the temperature field. An aim of this works is to determine the contact point of the tooth surfaces in an operate state in which the axes of rotors are skew. As a logical consequence of a change the curve contact in the point contact a change in the contact force an a gear ratio is shown. Own deformation of the screw rotors, consist in a force and temperature deformation [5] namely, is not involved into our solution.

2. Housing and rotors operational distortion

The force field of a screw compressor, which is considered at four time levels I, II, III, IV, before an opening of a discharge, determined by the angle $j_3 = \langle 0^{\circ},\ 18^{\circ}, 36^{\circ},\ 54^{\circ},\ 72^{\circ} \rangle \wedge 0^{\circ} \equiv 72^{\circ}$, of a rotary motion of the main rotor is given by pressure in chambers [3]. The value $j_3 = 0^{\circ}$, which conforms to the time level I and determines the beginning of the discharge, corresponds to a value of the angular displacement $j_{30} = 21{,}4^{\circ}$ from the starting position of rotors, Fig. 12. Separate working spaces with corresponding pressures in *MPa* for $j_3 = 0^{\circ}$ are marked in Fig. 2. Gas compression is described by adiabatic changes $pV^k = const.,\ k = 1{,}4$. Numerical solution was carried out for following geometric parameters: axes distance $a_w = 85\,mm$, gear ratio $i_{32} = 1{,}2$, helix angle on the rolling cylinders $g = 45^{\circ}$ and the length of a tooth part of rotors $l = 193{,}8\,mm$. The force field consist in a set of force and couple in nodes L_k of considered rotor axis, Fig. 3, is defined with relations $\mathbf{F}_K = \sum_{i=1}^{3} \mathbf{F}_{K_i}$, $\mathbf{M}_K = \sum_{i=1}^{3} \mathbf{M}_{K_i}$, where $\mathbf{F}_{K_i}, \mathbf{M}_{K_i}$, are results of the pressure on an elementary are a *i* of surfaces transformed in a node *k* of the rotor axis. Resultant of the elementary force effect, which is given with expressions $\mathbf{F} = \sum_{k=1}^{3} \mathbf{F}_K$, $\mathbf{M} = \sum_{k=1}^{n} \mathbf{r}_K \times \mathbf{F}_K$, are transferred to the housing by the bearings [3].

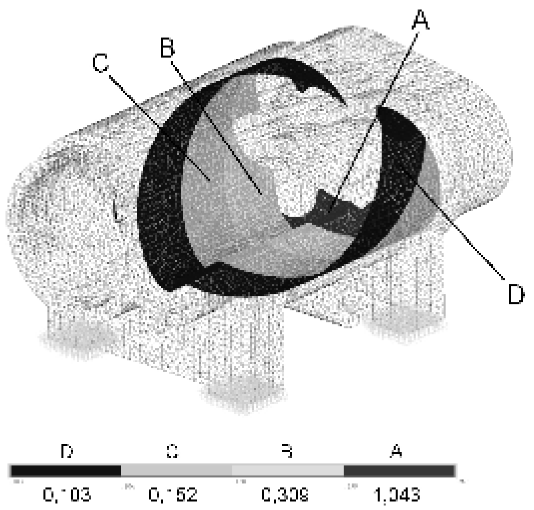

Fig. 2 Simplified model of screw machine housing with marked work spaces

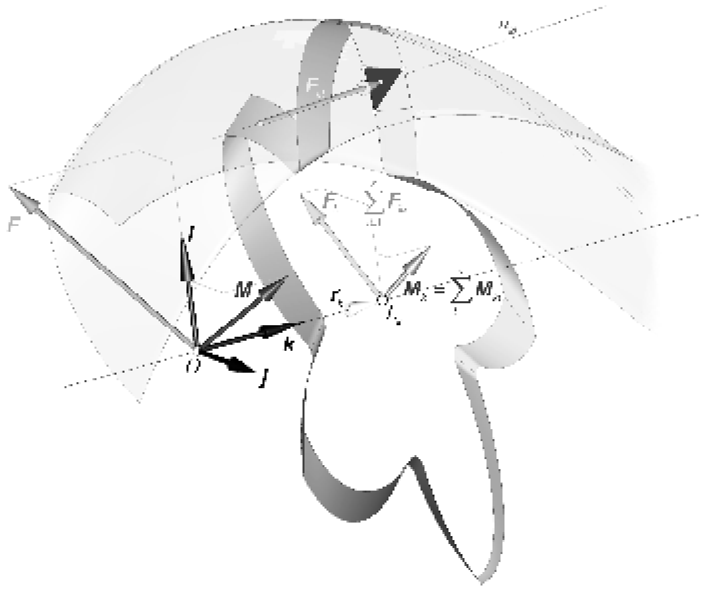

Fig. 3 Force effects on surface element

The temperature field was obtained by measurement and estimation. The distribution of the temperature field acting to the housing is presented in Fig. 4. Lower values was measured on the housing surface and upper values, which belong to the inner surface of the housing, were determined by estimation according to measured temperature of rotors. The distribution of the temperature field is constant along circumference in the frontal plane which is perpendicular to the rotor axes. A temperature measurement of rotors was made on the oil injected screw compressor [5], [6]. Temperature sensor was applied to rotors through drilled openings in the housing wall. Temperature distribution along the length of rotors is considered, see Fig. 4, according to a straight line. In a radial direction the temperature distribution is according to the straight as well. Force and heat housing deformation was determined separately using the software ANSYS and MSC.Marc. The total displacements of

Discharge pressure: $p = 7\,bar$

Revolution of the main rotor: $n = 4700\,rpm$

Injected oil quantity: $Q = 29\ \mathrm{l\,min^{-1}}$

Oil temperature: $t_0 = 60^{\circ}$

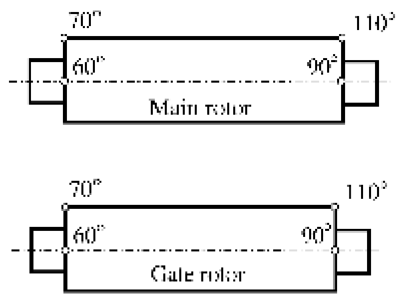

Fig. 4 Temperature field

bearing centres are presented in Tab. 1, [3], for position of rotor that is given by the angle of rotation $j_3 = 0^{\circ}$ of the main rotor that corresponds to the situation just before the opening of discharge. In this notation *A* determines bearing centres on the frontal and *B* on the back side of the housing.

Table 1: Displacement of bearing centre for $j_3 = 0^\circ$

Components	$\mathbf{r_{A3}}$	$\mathbf{r_{B3}}$	$\mathbf{r_{A2}}$	$\mathbf{r_{B2}}$
	[μm]			
Total displacement				
x	28,642	36,142	31,449	23,826
y	-10,600	-16,060	18,155	22,691
z	-55,597	54,396	-52,132	55,134

A visualization of total bearing displacements in four time levels I,II,III,IV is shown in Fig. 5, 6.

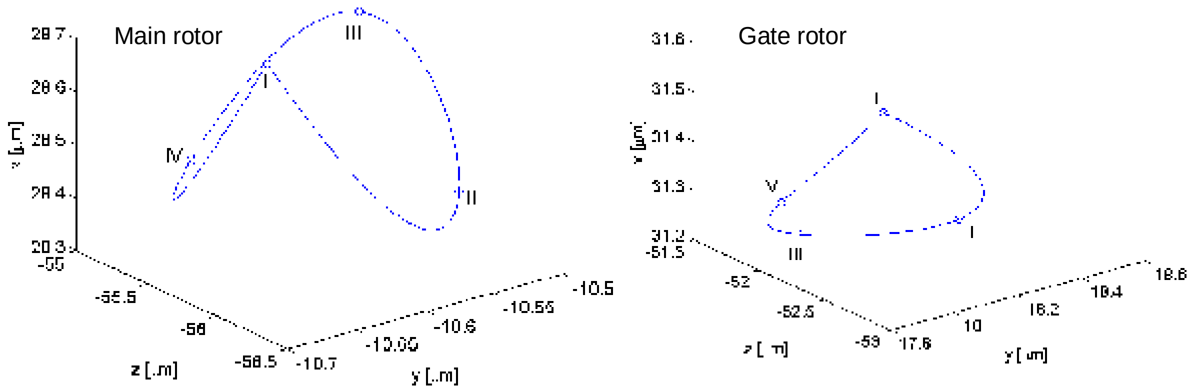

Fig. 5 Displacement of bearing centres situated on frontal side

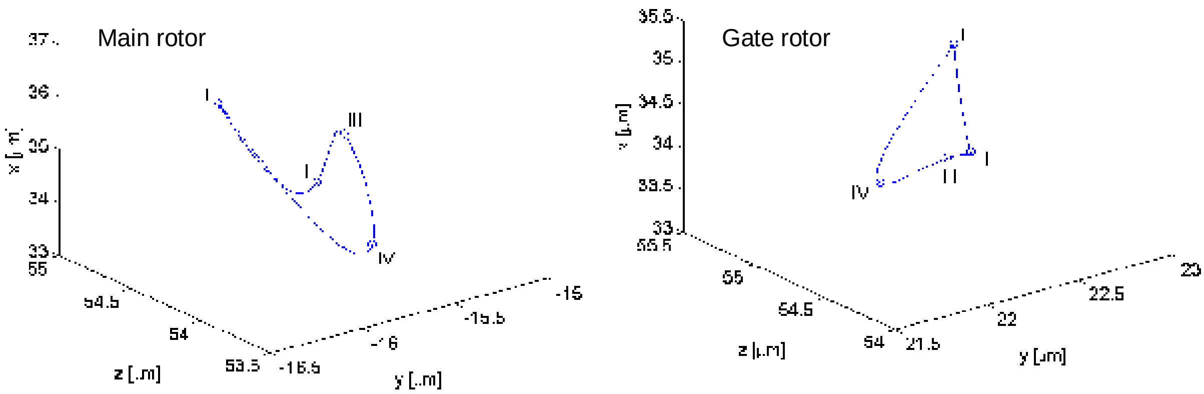

Fig. 6 Displacement of bearing centres situated on back side

3. Rotors in theoretic position

Tooth surfaces of the main and gate rotor create, Fig. 7, two conjugate surfaces where creating surface s_2, which is defined [4] by parametric equation

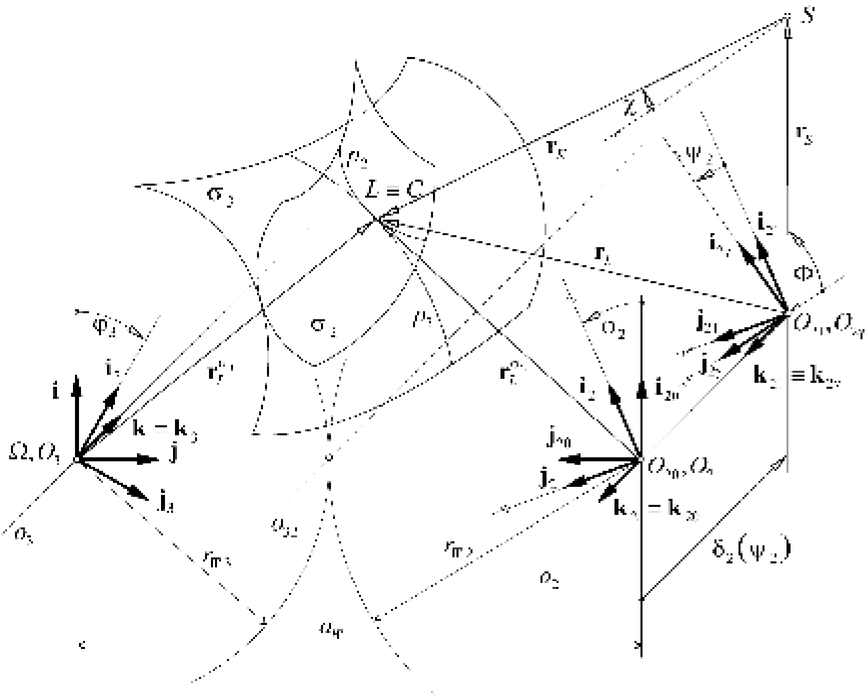

Fig. 7 Creating of conjugate tooth surfaces s_2 and s_3

$$
{}_{R_2}\mathbf{r}_L^{s_2}(y_2, c) = \begin{bmatrix} r_S \sin(f + y_2) - r_K \sin(c + y_2) \\ -r_S \cos(f + y_2) + r_K \cos(c + y_2) \\ d_2 \\ 1 \end{bmatrix} \tag{1}
$$

where ${}_{R_2}\mathbf{r}_L^{s_2}$ is the position vector of a point $L \in s_2$, $d_2 = r_{w2}\, y_2\, tgg$ is a displacement along the surface axis o_2, r_{w2} is the radius of the rolling cylinder, g is the helix angle on the rolling cylinder and r_S, r_K, f, c are geometric parameters. The conjugate surface s_3, which is an envelope of the creating surface s_2, is given by two equations

$$
{}_R\mathbf{r}_L^{s_3} = {}_R\mathbf{r}_L^{s_2} \wedge \mathbf{n}_L \cdot \mathbf{v}_{L_{32}} = 0 \tag{2}
$$

where ${}_R\mathbf{r}_L^{s_2}$ is the position vector of a point $L \in s_3$ in the basic coordinate system *R*, $\mathbf{n}_L$ is the normal vector of a common point $L \equiv L^{s_2} \equiv L^{s_3} \equiv C$ and $\mathbf{v}_{L_{32}}$ is the vector of the relative velocity in the point *L*. Using transformation matrices the first equation (2) can be written as

$$
{}_{R_3}\mathbf{r}_L^{s_3} = \mathbf{T}_{R,R_3}\ \mathbf{T}_{R_{20},R}\ \mathbf{T}_{R_2,R_{20}}\ {}_{R_2}\mathbf{r}_L^{s_2} \ . \tag{3}
$$

Substituting (1) to (3) we obtain

$$
{}_{R_3}\mathbf{r}_L^{s_3}(y_2, j_2, c) = \begin{bmatrix} r_S \sin(f + j_2 + j_3 + y_2) - r_K \sin(c + j_2 + j_3 + y_2) + a_w \sin j_3 \\ r_S \cos(f + j_2 + j_3 + y_2) - r_K \cos(c + j_2 + j_3 + y_2) + a_w \cos j_3 \\ d_2 \\ 1 \end{bmatrix}. \tag{4}
$$

The second equation (2) represents condition of perpendicularity of the normal vector $\mathbf{n}_L$ and the vector of the relative velocity $\mathbf{v}_{L_{32}}$ in the contact point $L \equiv C$ of the surfaces s_2 and s_3. The equation can be rewritten, in the case that the profile p_2 is created by an arc of a circle, into form

$$(i_{32}+1)\, r_K \sin(c - f) + a_w \sin(j_2 + c + y_{2L}) = 0 \tag{5}$$

where a_w is a distance between axes o_2, o_3 and $i_{32} = j_3 / j_2$ is a gear ratio. The equations (4) and (5) represent the surface s_3 meshing with the surface s_2. Both surfaces take the contact in a curve.

4. Rotors under operate state

An undeformed position of the rotors in the basic coordinate system $R \equiv (\mathbf{i}, \mathbf{j}, \mathbf{k})$, Fig. 7, is described with relations $\mathbf{r}_{O_3} = [0, 0, 0]^T$, $\mathbf{r}_{O_2} = [0, a_w, 0]^T$ and $\mathbf{v}_3 \equiv \mathbf{v}_2 = [0, 0, 1]^T$ where $\mathbf{v}_i$ is the unit vector of the rotor axis. The deformed position of the axes is caused by force and temperature loading of the housing and leads to a screw displacement of the axes. The skew arrangement is realized by following way, Fig. 8. The axis o_3 of the main rotor is fixed and

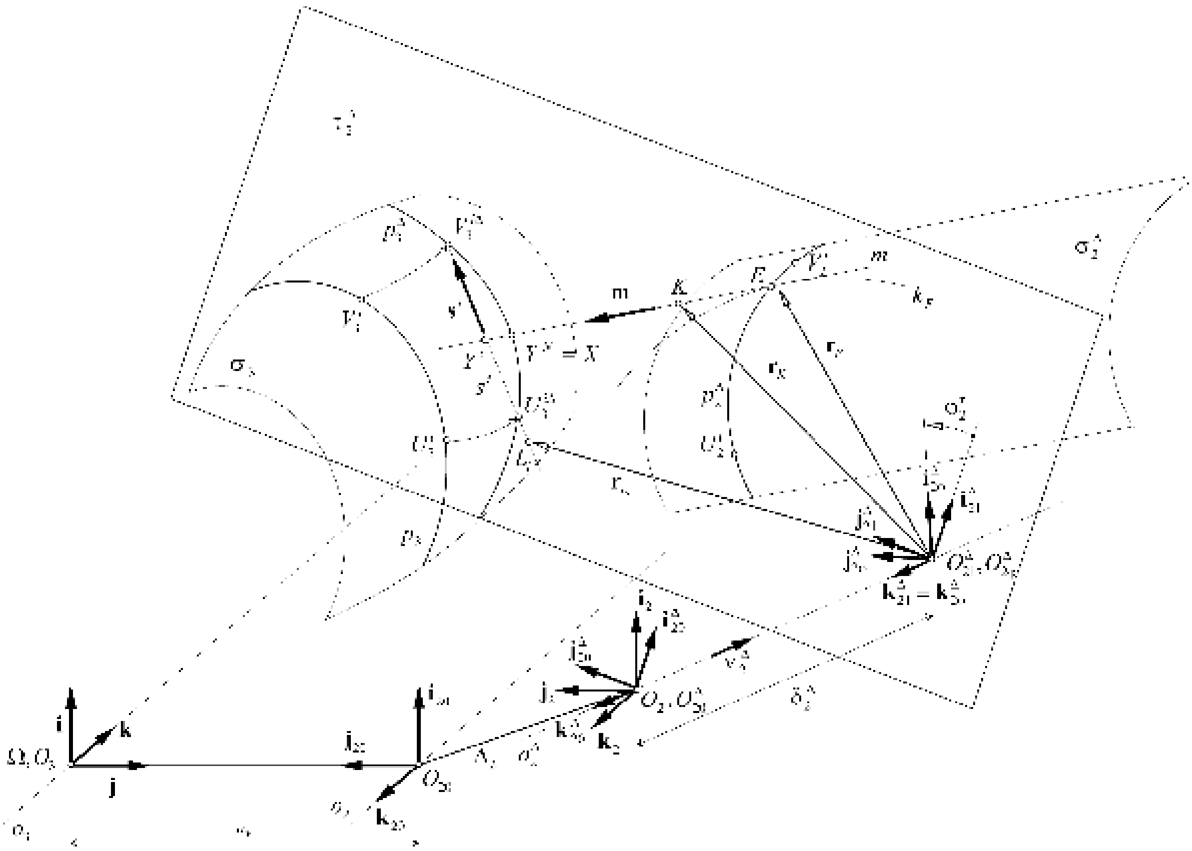

Fig. 8 Determination of contact point of profile p_3^{Δ} in cross section t_2^{D}

new, deformed, positions of axes o_2^D, o_3^D are inserted in the axis o_2. Then the deformed position s_2^D with the axis o_2^D represents a displacement of both surfaces. The displacement of the axis o_2 to the position o_2^D is given, Fig. 8, by the vector $\mathbf{\Delta}_2 = [2.8053,\ 28.7575, 3.4650]^T\ mm$, which determines a shift of the point O_{20} to the position O_{20}^D, and the unit vector $\mathbf{v}_2^D = \left[-1.5283 \cdot 10^{-5},\ 3.7011 \cdot 10^{-5},\ 0.9999\right]^T$ of the axis o_2^D for the first time level *I* ($j_3 = 0^{\circ}$). Time alternation of the vector $D_2(t)$ and unit vector $\mathbf{v}_2(t)$ of the axis o_2^D is shown in Fig. 9 where the individual time levels I ÷ IV are marked.

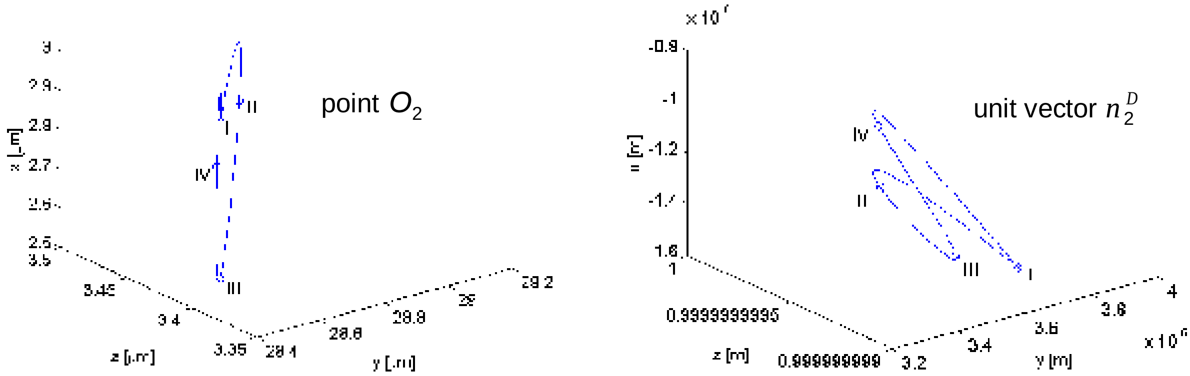

Fig. 9 Time displacement of point O_2 and vector of axis o_2^D

Contact point of surfaces s_3 and s_2^D we obtain using a set of cross sections t_2^D that give the set of separate single profiles p_2^D and p_3^D. Each of the profiles p_2^D rotates about the axis o_2^D, position of the surface $s_3 = \{ p_3^D \}$ is fixed, until it takes a contact with corresponding profile p_3^D. From the set of contact points X_j, $j = 1 \div n$, of the profile p_2^D and p_3^D, the contact point $L \equiv C$ of surfaces s_3 and s_2^D creates only this one that fulfils the condition $j_2^t = \min\{ j_{2j}^t \}$, where *j* denotes a cross section by the plane t_2^D, Fig. 8. In the contact point the normal of both surfaces must be coalesced, so the condition

$$\mathbf{n}_L^{s_2^D} \times \mathbf{n}_L^{s_3} = \mathbf{0} \tag{6}$$

must be fulfiled. Determination of the contact point between the profile p_2^D and p_3^D is made using a tangent *m* to the circle $k_E : O_{20}, r_E$, which originate by a rotary motion around the axis o_2^D, where $E = \{ L_j \}$is a chosen point of the profile p_2^D. Parametric equation of the tangent *m* to a circle k_E is given with equation

$$\mathbf{r}_K = \mathbf{r}_E + \mathbf{m}\ l \tag{7}$$

where **m** is the unit tangential vector of the tangent m and l is a searched parameter. The profile p_2^D is gradually turned, an angle j_2^t, until an equality $E \equiv X$ i.e. $\overline{Y^N E} \wedge \overline{Y^i Y^N} = 0$ takes place. Then $Y^N \equiv X$ is a contact point of profiles p_2^D and p_3^D. This algorithm is applied on all couples of curves $p_2^D \in s_2^D$ and $p_3^D \in s_3^D$. Profiles of considered tooth surfaces in the frontal section for $j_{30} = 0^\circ$ are shown in Fig. 10. Curves of the creating profile of the gate rotor are arcs of the circle k_1, k_3, k_7 and k_{11}, arc of the trochoid k_5 and the straight line k_9. A tooth profile of the main rotor consists of the curve $k_2, k_4, k_8, k_{10}, k_{12}$, which are envelopes of mentioned creating curves of the gate rotor. For contact analysis the meshing parts of profiles, which are defined by the curves k_7, k_9 and k_{11} on the gate rotor and the conjugate curves k_8, k_{10} and k_{12} on the main rotor, are considered.

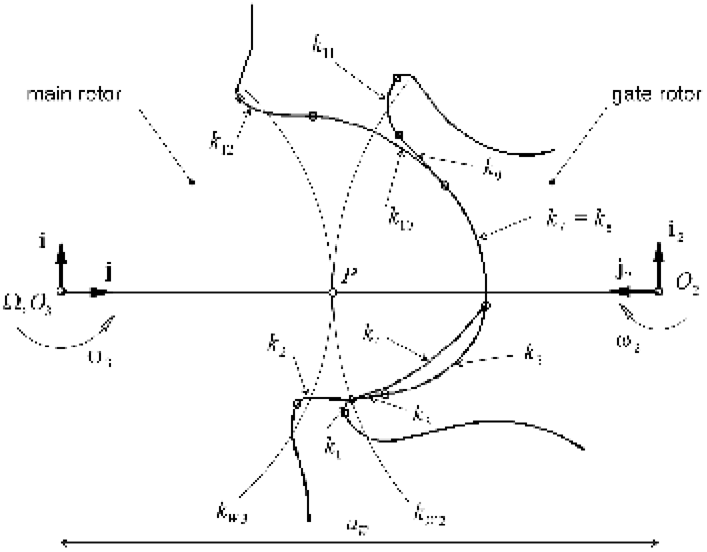

Fig. 10 Profiles of conjugate tooth surfaces

For an analysis of the contact of tooth surfaces s_2^D, s_3 during an operating cycle, which is given by a turning about one tooth pitch of the main rotor, the domain of definition of an angular displacement of the main rotor is $j_3 \in \langle 0^\circ, 72^\circ \rangle$.

Displacement of the contact point C of p-th pair of teeth on tooth surface s_3 of the main rotor, depending up time

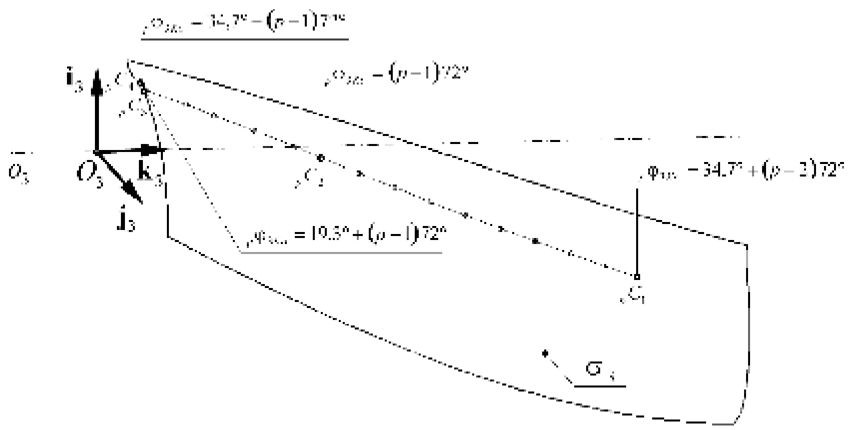

Fig. 11 Displacement of contact point of p-th pair of teeth on tooth surface of main rotor

level, is shown in Fig. 11. There ${}_pC_1$ is a point in which a contact of p-tth pair of tooth surfaces starts. The point ${}_pC_2$ determines the position in which the contact point conform to starting position of both surfaces, Fig. 10, by the surface creating. The point ${}_pC_3$ determines a location in which the contact point *C* over step to $p+1$ pair of surfaces.

5. Consequences

A change over a curve contact to contact at a point causes that a force transformation between rotors takes place at the point and not at a curve [3]. This fact is more important than a negligible difference between transmitted force effects. Already a small displacement of the rotor axes from parallel to skew position causes a significant increasing of a value of the normal force acting between tooth surfaces. Other consequence of a change of a contact character comes to a deviation of the gear ratio. Tooth surfaces s_2, s_3, which contact mutually in time *t* at a point *C*, have in this point common normal line *n*, Fig. 12. In the contact point following relations

$$\mathbf{n} \cdot \mathbf{v}_{32} = 0 \quad \wedge \quad \mathbf{n} \cdot \mathbf{v}_3 = \mathbf{n} \cdot \mathbf{v}_2 \tag{8}$$

have to be fulfilled. After substituting relation

$$\mathbf{v}_3 = \boldsymbol{\omega}_3 \times \left(\boldsymbol{\lambda}_3 + \boldsymbol{\kappa}_3 + \boldsymbol{\mu}_3\right), \qquad \mathbf{v}_2 = \boldsymbol{\omega}_2 \times \left(\boldsymbol{\lambda}_2 + \boldsymbol{\kappa}_2 + \boldsymbol{\mu}_2\right) \tag{9}$$

into the equation (8), multiplying and arrangement we can a momentary transmission ratio

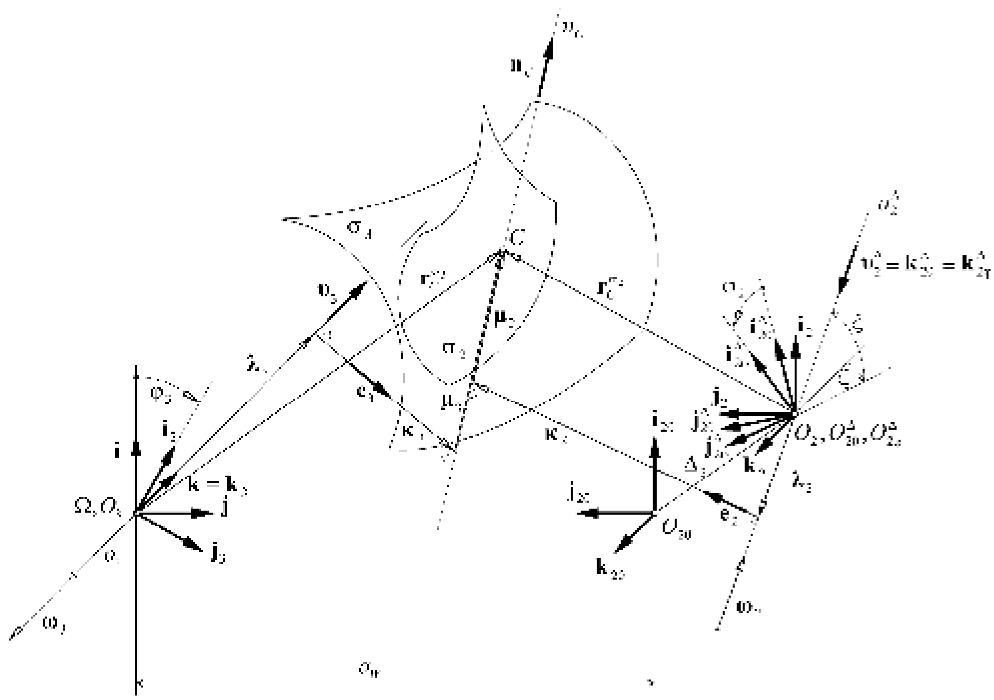

Fig. 12 Determination of instantaneous gear ratio

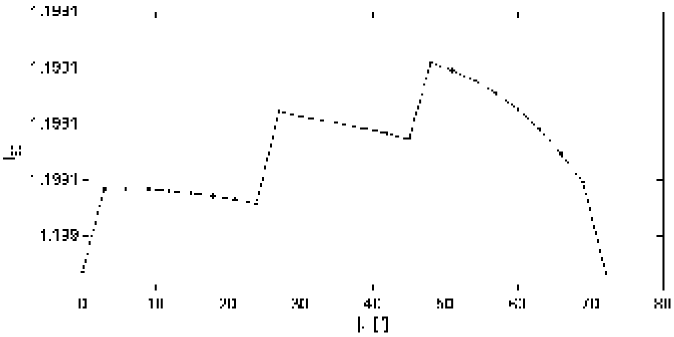

Fig. 13 Real gear ratio

determine as follows

$$i_{32} = \frac{w_3}{w_2} = \frac{k_2}{k_3}\frac{\sin n_2}{\sin n_3} \quad (10)$$

where

$$\sin n_2 = \frac{\mathbf{n} \cdot \boldsymbol{\omega}_i \times \boldsymbol{\kappa}_i}{w_i \; k_i} \; . \quad (11)$$

A graphic vizualization of the real gear ratio is shown in Fig. 13.

Conclusion

Heat and force loading of screw machines causes a distortion of their housing. In consequence of this deformation a parallel position of rotor axes changes into a skew position. An originally curve contact of tooth surfaces changes into a contact at a point. The change brings a local great contact loading of tooth surfaces and a deviation from the gear ratio. These influences induce probably a generation of operate vibration.

Acknowledgements

The work has been supported by the research project MSM 4977751303.

References

[1] Kameya, H., Aoki, M., Nozawa, S.: Three-dimensional curvature analysis on screw rotor and its applications. Proceedings of the International Conference on Compressors and their Systems 2005. London, John Willey & Sons, LTD, London 2005, pp. 467-474

[2] Stosic N. & Smith I. K. & Kovacevic A.: Screw Compressors. Springer Verlag. Berlin, Heidelberg, New York 2005

[3] Švígler J., Machulda, V., Siegl, J.: Deformation of Screw Machine Housing under Force Field and its Consequences. VDI Berichte Nr. 1932 Schraubenmaschinen 2006. Dortmund 2006, pp. 377-388

[4] Švígler J.: Incorrect contact of screw machine rotors. Proceedings of the International Conference on Compressors and their Systems 2005. London, John Willey & Sons, LTD, London 2005, pp. 3-12

[5] Švígler, J., Rinder, L.: Temperaturdeformation des wassereingespritzten, Schraubenkompressors. Schraubenmaschinen Nr. 13, Dortmund 2005, pp. 17-36

[6] Rinder, L., Moser, I.: Untersuchung der Olverteilung in den Arbeitsräumen nasslaufender Schraubenkompressoren. VDI Berichte Nr. 859. VDI Verlag, Düsseldorf 1990